

Cosmic-ray variation in local filamentary clouds

F.R. Kamal Youssef^{a,*} and I. A. Grenier^a for the *Fermi* LAT Collaboration

^a*Université Paris Cité and Université Paris-Saclay, CEA, CNRS, AIM,
91190 Gif-sur-Yvette, France*

E-mail: francois.kamalyoussef@cea.fr, isabelle.grenier@cea.fr

Observations by the *Fermi* Large Area Telescope (LAT) of nearby interstellar clouds have shown that the γ -ray emissivities measured per gas atom are fairly uniform within half a kiloparsec of the Sun, except in the Eridu cloud which exhibits a puzzling 30 – 50% drop in emissivity, hence in cosmic-ray flux. The magnetic field along this atomic filamentary cloud is largely ordered and points towards the halo, so cosmic rays may stream out towards high altitudes below the Galactic plane. To compare with the Eridu cloud, we have studied the γ -ray flux recorded in another nearby, highly-inclined, magnetically ordered, atomic filament named the Reticulum cloud.

We find a γ -ray emissivity in the Reticulum cloud that is fully consistent with the local average and that is 40-60% larger than in the similar Eridu cloud. We have studied the gas and magnetic-field states of these two clouds and we have derived estimates of the κ_{\parallel} diffusion coefficient parallel to the magnetic field in the self-confinement scenario where cosmic rays excite Alfvén waves via the streaming instability and those waves are damped by ion-neutral interactions. The equivalent κ_{\parallel} values we find in both clouds challenge the loss of cosmic rays in the Eridu filament.

38th International Cosmic Ray Conference (ICRC2023)
26 July - 3 August, 2023
Nagoya, Japan



*Speaker

1. Introduction

The Sun is located in a valley of low gas density surrounded by dense molecular clouds [1]. The γ -ray intensity produced by hadronic interactions between cosmic rays (CRs) and the interstellar gas in and around the valley has been recorded at energies above 30 MeV by the Large Area Telescope (LAT) on board the *Fermi* Gamma-Ray Space Telescope. The γ rays serve to probe the CR flux in different locations and in different types of interstellar environments.

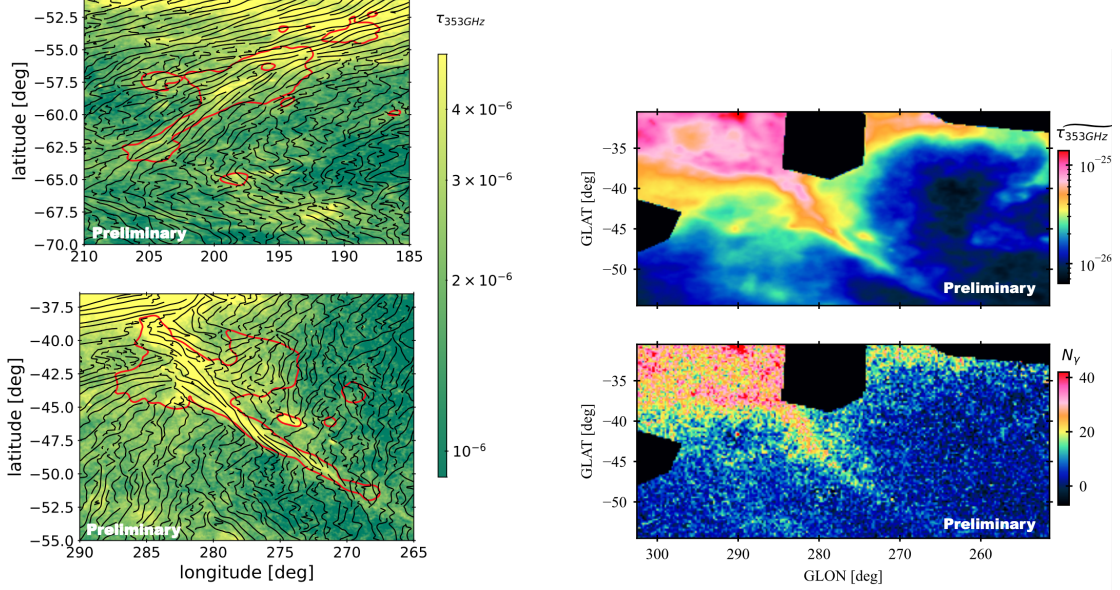
Given the current uncertainty in gas mass estimates in the CO-dark and CO-bright molecular phases of clouds, one can only infer the CR flux and spectrum with adequate precision in the atomic gas phase. Such a measurement exploits the spatial correlation between the γ -ray intensity and H I column density (N_{HI}) after correction for potential self absorption in H I line emission. The analysis requires maps of the other gas phases to avoid biasing the result on the H I correlation because a diffuse component is missing [2], but the component separation is robust if the different gas phases exhibit distinct spatial distributions. Spectra of the γ -ray emissivity per gas nucleon in the atomic phase, q_{HI} , are thus typically obtained at energies above a few hundred MeV to take advantage of the better angular resolution of the LAT to resolve nearby clouds.

Such emissivity measurements have been performed in different clouds of the local interstellar medium (ISM) (e.g. [2–5]) and the emissivity spectra appear to be very often consistent with the local average, $q_{\text{LIS}}(E)$, obtained for the whole atomic gas seen at Galactic latitudes ranging between 7° and 70° [3]. Such a consistency implies that the CR flux is rather uniform within a few hundred parsecs from the Sun [6]. One nearby cloud has, however, been found with a 34% lower γ -ray emissivity spectrum than the q_{LIS} average [5]. The statistically significant deviation (14σ) cannot be attributed to confusion with other clouds along the line of sight, nor to uncertainties in its H I mass because the lowest possible mass (optically thin H I lines) yields an upper limit to the q_{HI} emissivity that is still significantly 25% below q_{LIS} . The multi-GeV CRs probed by the LAT penetrate the cloud without hindrance given the modest column and volume densities of the diffuse gas [7]. The Eridu cloud therefore appears to be pervaded by a $\sim 30\%$ lower CR flux, but with the same particle energy distribution as in the local ISM.

The Eridu cloud is an atomic filament that is largely inclined with respect to the Galactic plane. It lies near the edge of the Orion-Eridanus superbubble at a distance of about 300 pc [8], at high Galactic latitudes and at an altitude of about 200-250 pc below the Galactic plane. The dust polarisation data at 353 GHz from *Planck* [9] shows that the magnetic-field lines are well-ordered and aligned with the filament axis (see Fig. 1a). The nearby Reticulum cloud presents gaseous and magnetic characteristics comparable to those of Eridu: it is also an atomic filament lying at the edge of the Local Valley, at a distance of about 240 pc [8]. Its ordered magnetic field runs parallel to the filament axis towards the south Galactic halo (see Fig. 1a). We have therefore measured the γ -ray emissivity spectrum per gas nucleon in this filament to compare it with the average in the local ISM and with the low emissivity spectrum of the Eridu cloud.

2. Data and Models

We have selected an analysis region around the Reticulum filament extending from 251.5° to 302.5° in Galactic longitude and from -54.5° to -30.5° in Galactic latitude, as shown in Fig. 1b. We



(a) Dust optical depth τ_{353} at 353 GHz in Galactic coordinates toward the Eridu (top) and Reticulum (bottom) filaments. The black lines give the orientation of the plane-of-the-sky magnetic field inferred from the dust polarisation observations at 353 GHz and an angular resolution of $14'$ (FWHM) with *Planck*. The red contours delineate the filaments at H I gas column densities of $3 \times 10^{20} \text{ cm}^{-2}$ and $1.2 \times 10^{20} \text{ cm}^{-2}$, respectively.

(b) Top: dust optical depth measured at 353 GHz from *Planck* and IRAS data and displayed at the angular resolution of *Fermi*-LAT; Bottom: γ -ray photon counts produced by CR interactions with gas in the 0.16–63 GeV energy band after subtraction of point sources and other ancillary emissions. The black regions towards the Magellanic clouds and Gum nebula have been excluded from the analysis region.

Figure 1

have masked regions with large column densities from the Magellanic clouds and from the edge of the Gum Nebula.

2.1 Gas data

We have used the 21-cm Galactic All Sky Survey GASS III data [10] to map the neutral atomic hydrogen (H I) in the region with an angular resolution of $16.2'$. Following the method developed by [2], we have used the position in the sky and central velocity of the H I lines to identify seven nearby cloud complexes across the analysis region. In order to correct the H I intensity for potential self absorption, we have produced the N_{HI} map of each cloud for a set of uniform spin temperatures ranging from 100 K to 800 K and also for the optically thin case. We have used the same spin temperature for all clouds and we have let it vary when modelling the dust and γ -ray data.

Planck has detected no CO(1-0) intensity up to 1 K km/s in the region [11]. We have further used the strong spatial correlation seen in Fig. 1b between the γ -ray intensity and dust optical depth to extract gas column densities that are not traced by H I emission, but permeated by both CRs and dust grains. This dark neutral medium (DNM) corresponds to the H-H₂ transition where the dense

H α becomes optically thick to 21-cm line emission and CO emission is absent or too faint to trace the H $_2$ gas.

2.2 Dust data and model

We have used the all-sky map of the dust optical depth at 353 GHz (τ_{353}) to trace the dust column density ([12], updated by [13]). The map was constructed at an angular resolution of 5' by modelling the dust thermal emission recorded by *Planck* and *IRAS*. We have degraded the original resolution to that of the GASS H α survey to model the dust and gas correlations. The dust optical depth should linearly scale with the total gas column density, N_H , if the dust-to-gas mass ratio and grain emissivity remain rather uniform within a given cloud. The data support this assumption in atomic clouds [12]. We have therefore modelled $\tau_{353}(l,b)$ as a linear combination of the different gas contributions (N_{HI} and $N_{H_{DNM}}$) of the seven clouds, with free normalisations to be fitted to the data, as in [2]. A free isotropic term has been added to account for the residual noise and the uncertainty in the zero level of the dust maps. [12, 14]. The parameters have been estimated using a least-square χ^2 minimisation with a fractional error of 11% that yields a reduced χ^2 value of one in the dust fit. This error reflects the uncertainty in the model. The optical depth errors are smaller.

2.3 Gamma-ray data and model

We have used fourteen years of *Fermi*-LAT Pass 8 survey data for energies between 0.16 and 63 GeV and we have analysed the data in eight energy bands, bounded by $10^{2.2}$, $10^{2.4}$, $10^{2.6}$, $10^{2.8}$, $10^{3.0}$, $10^{3.2}$, $10^{3.6}$, $10^{4.0}$, and $10^{4.8}$ MeV. We have applied tight selection criteria for the photon types and arrival directions to keep the contamination by residual CRs and by Earth atmospheric γ rays to less than 10%. We have also combined photons of different PSF types in each energy band to obtain a PSF 68% containment radius of 2.1° in the lowest energy bin and close to 1° in all the other energy bands. The resulting photon map is shown in Fig. 1b where we have subtracted the point sources and the smooth isotropic and inverse-Compton emissions to display the γ rays produced in the clouds.

Multi-GeV CRs easily propagate through the different gas phases, so the γ -ray emission can be modelled, to first order, by a linear combination of the gas column densities in the H α and DNM phases of the seven clouds. The model also includes a contribution from the Galactic inverse-Compton intensity modelled by GALPROP¹, point sources of non-interstellar origin from the 4GFL-DR3 catalogue [15], and an isotropic intensity² to account for the extragalactic γ -ray background and for CRs misclassified as γ rays.

In order to compare the model with the LAT photon data in each energy band, we have applied the energy-dependent instrument response functions (exposure, PSF, energy resolution) to each emission component and we have summed the photon count maps for the different combinations of PSF types to match the photon selection in the data. We have used a binned maximum-likelihood with Poisson statistics to fit the model coefficients to the LAT data in each of the eight energy bands.

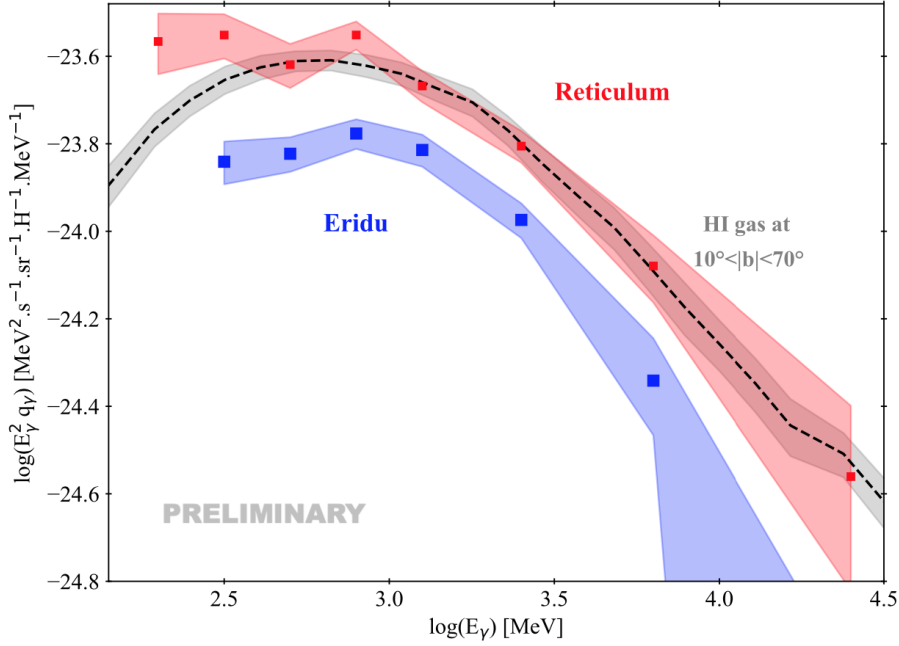


Figure 2: Spectral evolution of the γ -ray emissivities per gas nucleon in the Eridu (blue) and Reticulum (red) clouds. The grey curve gives the average q_{LIS} emissivity measured in the local ISM [3]. The emissivities are shown for the HI optical-depth correction that best fits the γ -ray data ($T_s = 100$ K for Eridu, 140 K for q_{LIS} , and optically thin for Reticulum). The shaded bands include the statistical and systematic uncertainties.

3. Results

Figure 2 compares the γ -ray emissivity spectrum we have found per gas atom in the Reticulum filament to that in Eridu and to the average q_{LIS} spectrum measured in the local ISM, at latitudes between 10° and 70° across the sky [3]. To compare the clouds we have plotted the emissivities obtained for the HI spin temperatures that best fit their respective γ -ray data. We can see that the CR population that permeates the HI phase of Reticulum has the same energy distribution and same flux as the average CR population in the local ISM.

On the other hand, the CR flux pervading Reticulum is 1.57 ± 0.09 larger than in Eridu despite their structural, gaseous, and magnetic similarities. This discrepancy decreases to 1.51 ± 0.09 if we compare them for the same HI spin temperature of 100 K and to 1.38 ± 0.08 if we assume them both to be optically thin to HI emission. The shape of the emissivity spectrum is preserved between the two clouds, which implies that the loss mechanism that affects CRs in Eridu must be energy independent.

¹<http://galprop.stanford.edu>

²<http://fermi.gsfc.nasa.gov/ssc/data/access/lat/BackgroundModels.html>

4. Diffusion characteristics

The Reticulum and Eridu clouds are both filamentary clouds, with ordered magnetic fields on the scales of several parsecs and with a large inclination with respect to the Galactic plane, reaching out to $z = 200 - 250$ pc below the plane. They both stand near the rim of the Local Valley, albeit on opposite sides. Yet, half as many CR nuclei propagate through Eridu compared to Reticulum.

Theory suggests that CRs in the GeV to TeV momentum range probed by the LAT observations primarily diffuse on self-excited magnetohydrodynamics turbulence [16]. CRs with a bulk drift speed, v_D , greater than the ion Alfvén speed, $v_A^{ion} = B/\sqrt{4\pi\rho_i}$, can excite Alfvén waves with the growth rate [17]:

$$\Gamma_g(k) = \frac{\pi^{3/2}}{2} \frac{e}{c} (v_D - v_A^{ion}) \frac{1}{\sqrt{\rho_i}} \sum_j \frac{\alpha_j - 3}{\alpha_j - 2} Z_j n_j(\mathcal{R}_j > \frac{B}{k}) \quad (1)$$

where ρ_i notes the mass density of interstellar gas ions, B is the mean field strength, and we add the contributions of different CR nuclei with charge $Z_j e$, rigidity \mathcal{R}_j above the gyro-resonance condition $\mathcal{R}_j = B/k$, and with volume number density spectrum $n_j(\mathcal{R})$ with a power-law spectral index α_j in the range of interest. We have considered the spectra of CR nuclei with $Z_j \leq 28$ incident on the heliopause [18]. They correspond to the average q_{LIS} emissivity discussed above. We have integrated the spectra over 1 GV in rigidity and fitted the α_j spectral indices in the 1-20 GV range that contributes most to the growth rate. The net drift with respect to the Alfvén wave frame can be written as a diffusive flux [19]: $v_D - v_A^{ion} = \kappa_{\parallel}/\ell_{CR}$ with a diffusion coefficient κ_{\parallel} parallel to the mean B field and a typical CR scale length ℓ_{CR} that we set to 200 pc given the distance that separates the deviant Eridu cloud from surrounding clouds exhibiting the average q_{LIS} spectrum.

The scattering rates are limited by wave damping. The latter arises primarily from interactions between ions and neutrals in the neutral gas phases that we have probed in γ rays [20]. Momentum exchange between the ions and H or He neutral atoms, with the same equilibrium temperature T , leads to the damping rate $\Gamma_{\text{in}} = \frac{4}{3} \frac{n_{\text{HI}}}{\sqrt{A_i m_H}} \sqrt{\frac{2}{\pi} k_B T} \left[\sigma_{iH} \sqrt{\frac{1}{1+A_i}} + x_{\text{He}} \sigma_{iHe} \sqrt{\frac{A_{\text{He}}}{A_i + A_{\text{He}}}} \right]$ given by [21], where k_B is the Boltzmann constant, $A_{\text{He}}=4$ is the He atomic weight, and $\sigma_{iH} = 10^{-14}$ cm² and $\sigma_{iHe} = 3 \times 10^{-15}$ cm² are the ion-H and ion-He momentum-transfer cross sections [22]. The interstellar helium abundance is $x_{\text{He}} = n_{\text{He}}/n_{\text{HI}} = 0.085$ by number [23]. The ion abundance and mean ion atomic weight, A_i , vary with the gas state. In the lukewarm and cold atomic phases prevailing along both clouds, the dominant ions are about half H⁺ and half C⁺, so $A_i \approx 6.5$. We have used the local-ISM version of the cooling, heating, and ionisation model of [24] to infer the temperature and ionisation fraction $x_i = n_i/n_{\text{HI}}$ as a function of the total gas density.

A quasi-steady state is reached when the growth rate Γ_g of the gyro-resonant waves is balanced by the damping rate Γ_{in} , yielding a parallel diffusion coefficient:

$$\kappa_{\parallel} = \frac{2}{\pi^{3/2}} \frac{c}{e} \Gamma_{\text{in}} \ell_{CR} \frac{\sqrt{\rho_i}}{\sum_j \left(\frac{\alpha_j - 3}{\alpha_j - 2} \right) Z_j n_j(\mathcal{R}_j > \frac{B}{k})} \quad (2)$$

In order to estimate the H I gas volume density in the clouds, we have used two different assumptions for the cloud geometry: a cylindrical fiber or a shell seen edge on. In the first geometry, the line-of-sight depth is close to the observed width in the plane of the sky, which we

estimate to be 5 ± 1 pc for Reticulum and 11 ± 4 pc for Eridu. In the shell geometry, depth estimates of 20 pc for Reticulum and 30 pc for Eridu give approximate upper limits to the cloud depths. We have found volume densities all along the Eridu filament that, in both geometries, are typical of the unstable lukewarm neutral medium that transitions between the stable warm and cold atomic phases. Gas densities along the Reticulum filament are ten times denser and typical of the cold neutral medium, in agreement with the detection of dark neutral gas at the atomic to molecular transition in this cloud. Hence dense cooling clumps are present inside both clouds, but they are more numerous and densely packed in Reticulum than in Eridu.

Table 1: κ_{\parallel} diffusion coefficients in $\text{cm}^2 \text{s}^{-1}$, obtained for the same CR flux pervading the two clouds and for different cloud geometries.

	cylindrical fiber	edge-on shell
Reticulum	$(4 \text{ to } 7) \times 10^{28}$	$(3 \text{ to } 4) \times 10^{28}$
Eridu	$(3 \text{ to } 4) \times 10^{28}$	$\sim 3 \times 10^{28}$

For the same CR flux propagating through the clouds, the results in Table 1 indicate that the denser neutral environment that characterises the Reticulum cloud yields only slightly larger diffusion coefficients along the mean magnetic field as the ion-neutral damping is more severe. On the other hand, the fact that the CR flux pervading Eridu is lower than in Reticulum implies a slower wave growth and faster diffusion. Increasing the Eridu κ_{\parallel} values of Table 1 by the CR flux ratio of 1.57 ± 0.09 yields equivalent coefficients of order $(4 \text{ to } 7) \times 10^{28} \text{ cm}^2 \text{ s}^{-1}$ in both clouds. From self-confinement theory, one would expect CRs to stream at about the same speed along and out of both filaments, so the comparative loss of CRs in Eridu challenges the average transport properties inferred at a parsec scale from the observations. These two clouds provide an important test case to further study how magnetic-field line tangling and ion-neutral damping regulate the diffusion of streaming CRs in weakly ionised gas at the few micro-parsec scale of gyro-resonance.

References

- [1] Leike, R. H., Glatzle, M., & Ensslin, T. A. 2020, A&A, 639, A138
- [2] Planck Collaboration, Fermi Collaboration, Ade, P. A. R., et al. 2015, A&A, 582, A31
- [3] Casandjian, J.-M. 2015, ApJ, 806, 240
- [4] Remy, Q., Grenier, I. A., Marshall, D. J., & Casandjian, J. M. 2017, A&A, 601, A78
- [5] Joubaud, T., Grenier, I. A., Casandjian, J. M., et al. 2020, A&A, 635, A96
- [6] Grenier, I. A., Black, J. H., & Strong, A. W. 2015, ARA&A, 53, 199
- [7] Joubaud, T., Grenier, I. A., Ballet, J., & Soler, J. D. 2019, A&A, 631, A52
- [8] Kamal Youssef, F. R. and Grenier, I. A. , 2023, A&A, in preparation.
- [9] Planck Collaboration, Ade, P. A. R., Aghanim, N., et al. 2015, A&A, 576, A104

- [10] Kalberla, P. M. W. & Haud, U. 2015, *A&A*, 578, A78
- [11] Planck Collaboration, Ade, P. A. R., Aghanim, N., et al. 2014, *A&A*, 571, A13
- [12] Planck Collaboration, Abergel, A., Ade, P. A. R., et al. 2014, *A&A*, 571, A11
- [13] Irfan, M. O., Bobin, J., Miville-Deschênes, M.-A., & Grenier, I. 2019, *A&A*, 623, A21
- [14] Casandjian, J.-M., Ballet, J., Grenier, I., & Remy, Q. 2022, *ApJ*, 940, 116
- [15] Abdollahi, S., Acero, F., Baldini, L., et al. 2022, *ApJS*, 260, 53
- [16] Amato, E. & Blasi, P. 2018, *Advances in Space Research*, 62, 2731
- [17] Kulsrud, R. M. & Cesarsky, C. J. 1971, *Astrophys. Lett.*, 8, 189
- [18] Boschini, M. J., Della Torre, S., Gervasi, M., et al. 2020, *ApJS*, 250, 27
- [19] Hopkins, P. F., Squire, J., Chan, T. K., et al. 2021, *MNRAS*, 501, 4184
- [20] Xu, S. & Lazarian, A. 2022, *ApJ*, 927, 94
- [21] Soler, R., Terradas, J., Oliver, R., & Ballester, J. L. 2016, *A&A*, 592, A28
- [22] Vranjes, J. & Krstic, P. S. 2013, *A&A*, 554, A22
- [23] Asplund, M., Grevesse, N., Sauval, A. J., & Scott, P. 2009, *ARA&A*, 47, 481
- [24] Kim, J.-G., Gong, M., Kim, C.-G., & Ostriker, E. C. 2023, *ApJS*, 264, 10